International Journal of Coal Geology 119 (2013) 177–186

Contents lists available at ScienceDirect

International Journal of Coal Geology

journal homepage: www.elsevier.com/locate/ijcoalgeo

Late Paleozoic continental warming of a cold tropical basin and floristic change in western Pangea

Neil J. Tabor [a,*], William A. DiMichele [b], Isabel P. Montañez [c], Dan S. Chaney [b]

[a] Huffington Department of Earth Sciences, Southern Methodist University, PO Box 750395, Dallas, TX 75275-0395, United States
[b] Department of Paleobiology, NMNH Smithsonian Institution, Washington, DC 20560, United States
[c] Department of Earth and Planetary Sciences, 2119 Earth and Physical Sciences, University of California, Davis 95616, United States

ARTICLE INFO

Article history:
Received 3 June 2013
Received in revised form 10 July 2013
Accepted 11 July 2013
Available online 21 July 2013

Keywords:
Pennsylvanian
Permian
Paleoclimate
Paleobotany
Paleotemperature
Biological diversity

ABSTRACT

An increase in mineral crystallization temperatures of ~13 ± 3 °C is preserved in paleosol profiles (ancient soils) within a stratigraphic interval of <40 m thickness in Permo-Carboniferous strata in western equatorial Pangea (modern north-central Texas). Late Pennsylvanian and Early Permian soil-mineral crystallization temperatures are estimated through the study interval with oxygen and hydrogen isotope compositions of paleopedogenic phyllosilicates and hematites taken from paleosol profiles. Considering monthly soil- and air-temperature measurements from modern equatorial Africa, phyllosilicate crystallization temperatures likely exceed surface air temperatures by ~2 ± 2 °C. Furthermore, the warming trend emerges from Pennsylvanian-age soil mineral crystallization temperatures, which are substantially *cooler* than soil temperatures observed in the modern lowland tropics, to Permian-age soil mineral crystallization temperatures, which are equivalent to, or slightly exceed, soil temperatures observed in modern lowland tropics. This record of mineral crystallization temperatures occurs at a time when some sources indicate the onset of the largest single glaciation of the Late Paleozoic Ice Age.

The temperature change indicated by these paleosol minerals is accompanied by a unidirectional, irreversible change in the composition of tropical lowland vegetation. This transition delineates the magnitude and characteristics of vegetational changes in the modern tropics that might accompany continued atmospheric warming. Times of low surface temperatures coincide with a typical Late Pennsylvanian, tropical Pangean, "wet" biome dominated by *Sigillaria*, *Macroneuropteris*, other pteridosperms and marattialean ferns. This plant assemblage is replaced spatially by a xeromorphic biome dominated by conifers, callipterids, and other seed plants, characteristic of the tropical Permian across western and central Pangea. The fully xeromorphic flora appears initially in sub-meter-scale beds within outcrops otherwise characterized by wet flora, and becomes predominant once peak surface temperatures were reached in the earliest Permian. A narrow stratigraphic interval (20 m) separates these two biomes in the region, marking what was to be a permanent floristic change in western Pangea. The lower diversity floras of seasonally dry habitats apparently migrated from drier extrabasinal areas into increasingly dry landscapes formerly dominated by the wet biome. This study documents the regional disappearance of an entire tropical biome with a net reduction of biodiversity accompanying rapid environmental warming.

1. Introduction

There is considerable evidence from the Quaternary ice ages to suggest rapid vegetational responses of large magnitude and over great spatial extent to changes in climate accompanying glacial–interglacial cycles, both in tropical and temperate regions (e.g., Bush et al., 2007; Colinvaux et al., 1996; Urrego et al., 2009; Webb et al., 2003; Williams et al., 2010). Similarly, but deeper in time, major changes in the spatial distribution of Cenozoic floral composition and diversity have been shown to correlate closely with changes in global temperature. For example, during the Paleocene–Eocene Thermal Maximum (PETM) (McInerney and Wing, 2011), a spike of warming in an already warm world, a correlation has been documented between floristic extinction (or major extirpation) and rapid, short pulses of global warming of ~5 °C, both in the tropics (Jaramillo et al., 2006) and mid-latitudes (Wing et al., 2005).

The generality of these kinds of plant responses is demonstrated by still older vegetational dynamics, recorded during the last cold-Earth interval before the present one, the Late Paleozoic Ice Age (LPIA). At this time ecosystems were populated by very different plants from those that have dominated Cenozoic landscapes (e.g., Boyce et al., 2010; Gastaldo et al., 1996; Pfefferkorn et al., 2008), and the Earth's continents were initiating the assembly of the supercontinent of Pangea. There were nonetheless rapid and spatially extensive responses to changing global climates driven by changes in the volume of polar ice at multiple

* Corresponding author. Tel.: +1 214 768 4175; fax: +1 214 768 2701.
E-mail address: ntabor@smu.edu (N.J. Tabor).

0166-5162/$ – see front matter © 2013 Elsevier B.V. All rights reserved.
http://dx.doi.org/10.1016/j.coal.2013.07.009

spatial and temporal scales (Fielding et al., 2008; Isbell et al., 2012; Montañez and Poulsen, 2013).

Here we examine vegetational changes in western equatorial Pangea across the Pennsylvanian–Permian boundary during the LPIA. This was a time interval during which a major pulse of southern hemisphere ice has been proposed, possibly the largest glacial advance of the LPIA (Fielding et al., 2008; Isbell et al., 2003; Koch and Frank, 2011). During this time interval a major vegetational change occurred, from floras characteristic of "wet" habitats to those typical of seasonally dry habitats (DiMichele et al., 2006; Montañez et al., 2007; Opluštil, 2013). This change parallels similar shifts in vegetation throughout central and western Pangea during this time (Broutin et al., 1990; DiMichele and Aronson, 1992; Kerp, 1996), and occurs contemporaneously with the changes in vegetation documented in Dunkard strata of eastern North America (DiMichele et al., 2013; Eble et al., 2013).

In the study area of north-central Texas, the sequence of lithologic and floristic changes begins with a thick (>200 m) stratigraphic interval containing coals and coaly shales dominated by "wet" floras with a few intercalated "dry" floras. This is succeeded by a <40 m thick mudstone-dominated interval with a mixed transitional flora of plants characteristic of both "hygromorphic" (wet-adapted) and "xeromorphic" (dry-adapted) species. The mixed floristic zone is followed by >600 m of red-to-gray mudstone dominated by xeromorphic floral elements. There is no evidence of a major hiatus within these strata (Hentz, 1988; Tabor and Montañez, 2004; DiMichele et al., 2006) or in biostratigraphically correlative marine strata (Dunbar and Committee on Stratigraphy, 1960; Wardlaw, 2005) to the southwest. The biological changes that occur through this interval appear to reflect directionally changing climate, independently assessed by the study of paleosol morphologies and light stable isotopic compositions of pedogenic minerals (Nelson et al., 2001; Tabor, 2007; Tabor and Montañez, 2004, 2005; Tabor et al., 2002). These physical climate proxies document a change from humid "ever wet" conditions in the Pennsylvanian, to progressively drier, seasonal climates across the Pennsylvanian–Permian boundary, to highly seasonal monsoonal and drier climate patterns persisting at least through the early Middle Permian in western equatorial Pangea (DiMichele et al., 2006; Tabor and Montañez, 2002, 2004; Tabor et al., 2002).

An estimated change, from ~22 ± 3° to ~35 ± 3 °C, in crystallization temperatures of phyllosilicates and hematites is preserved in paleosol profiles through the Pennsylvanian–Permian transition in the study area (Tabor, 2007; Tabor and Montañez, 2005). Yet, it is unclear how these soil temperature estimates relate specifically to contemporaneous surface air temperatures. While recent isotopologue measurements of CO_2 from soil calcite provide indications of a seasonal bias toward the warm season and thus yield crystallization temperatures substantially higher than mean annual air temperatures, previous studies of the stable isotope composition of soil-formed phyllosilicates and oxyhydroxides in the tropics of the present day have been interpreted to provide indications of mean climatic conditions within the soil (Giral-Kacmarcik et al., 1998; Yapp, 1990). Furthermore, it is well known that mean soil temperatures are typically >1 °C warmer than corresponding mean surface air temperatures (Buol et al., 2003). Temperature data from analogous modern tropical soils from equatorial Africa are presented here in order to provide a context for these Pennsylvanian–Permian soil temperature estimates, their relationship to surface air temperatures, and the potential impact it had on vegetation.

It is unclear whether tropical temperature change was the driving force for, or an outcome of, the collapse of the tropical ever wet biome in the Late Pennsylvanian. Nevertheless, this temperature change would have affected floral composition by introducing new environmental stresses, such as vast increases in the proportions of soil moisture lost through evapotranspiration (Jipp et al., 1998).

2. Geologic and stratigraphic framework

The Pennsylvanian–Permian transition on the NE Shelf of the Midland Basin, north-central Texas (98–99° W, 32–33° N; Fig. 1A) is within the Markley Formation, which is dominantly composed of mudstones, coals/organic shales, and numerous, laterally traceable sandstone beds (Hentz, 1988; Wardlaw, 2005). The succeeding Archer City and Nocona formations, which are Early Permian in age (Fig. 1B), are composed dominantly of mudstone with channel-form sandstone bodies (Tabor and Montañez, 2004). Mudstones of all three formations preserve morphological evidence of significant pedogenic modification soon after deposition (DiMichele et al., 2006; Tabor and Montañez, 2004).

The exact placement of the Pennsylvanian–Permian boundary within the continental strata of north-central Texas is not precisely known. The Markley Formation is broadly correlative to the largely marine Harpersville and Pueblo formations to the south (Hentz, 1988; Wardlaw, 2005). Conodont biostratigraphy of intercalated marine rocks in the Harpersville and Pueblo formations (Wardlaw, 2005) places the boundary between the Stockwether Limestone, in which *Streptognathodus isolatus* first occurs, the conodont marker for the base of the Permian, and the Saddle Creek Limestone of the Harpersville Formation, which can be projected into the uppermost part of the large terrestrial Markley Formation, based on the mapping of sandstone packages by Hentz and Brown (1987). This suggests that (i) the Gzehlian–Asselian (Permian–Carboniferous) boundary lies a short distance beneath the Markley–Archer City formation boundary within the study area and (ii) sedimentation was relatively continuous, with no significant hiatus, between Upper Pennsylvanian and Permian strata of the study area (Fig. 2). Thus, the lithological changes, estimated temperature increase, and floristic change are defined from the same stratigraphic succession, through the Permian–Pennsylvanian transition.

Lucas (2006, p. 70) recommended combining the Nocona and Archer City formations based on their conformability and difficulty to distinguish the two units while mapping; there is insufficient lithological difference to make them differentiable in the field, the principal criterion for formational status. We have continued to use both Archer City and Nocona formations in this contribution for consistency with other empirical studies the authors have published on these units, recognizing that in the future adjustments will be necessary. The sections described here correlate with the Coyotean and Seymourian vertebrate faunachrons of Lucas (2006); the Pennsylvanian–Permian boundary is located in the lower 1/3 of the Coyotean faunachron.

3. Materials and methods

3.1. Geochemical methods and background data

The methods employed for geochemical analyses and development of mineral-crystallization temperature estimates are provided in detail elsewhere (Tabor, 2007; Tabor and Montañez, 2005; Tabor et al., 2002). A brief description of geochemical methods is provided here. Paleopedogenic phyllosilicates and hematites were selected from 3 localities in the Gzhelian–Asselian-age Markley Formation, and from 6 different localities in the Asselian–Sakmarian-age Archer City and Nocona formations from among dozens of documented paleosol occurrences (DiMichele et al., 2006; Tabor, 2007; Tabor and Montañez, 2002, 2004, 2005; Tabor et al., 2002; Table 1). Bulk samples were collected in the field and pedogenically-derived mineral fractions were isolated from them and analyzed for isotopic composition (Tabor, 2007; Tabor and Montañez, 2005; Tabor et al., 2002). Pedogenic phyllosilicate minerals were characterized by X-ray diffraction; the relative concentration and chemical composition of phyllosilicate minerals in each sample were determined by FTIR and electron microprobe analyses (Tabor and Montañez, 2005). Phyllosilicate oxygen and hydrogen isotope fractionation equations were calculated using the bond-model approach

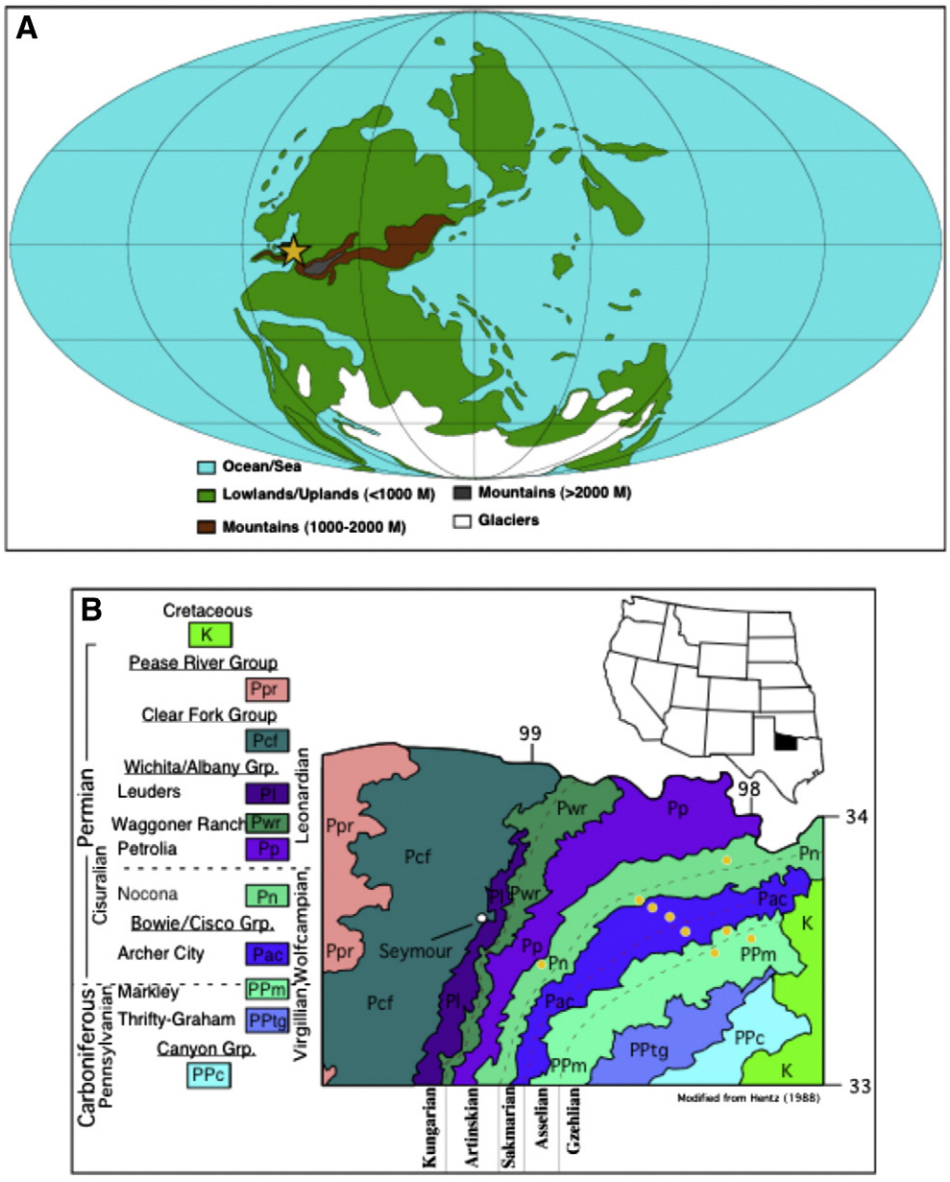

Fig. 1. (A) Paleogeographic reconstruction of Early Permian (Sakmarian) time showing the major oceans and seaways (blue areas), tectonic elements (brown and gray areas) and geomorphological elements of continental ice (white areas) on Earth. The paleogeographic position of the north Texas, USA study area is demarcated by the yellow star. Modified from Ziegler et al. (1997). (B) Stratigraphic chart (left) and regional distribution of stratigraphic units (right) in the north Texas, USA study area. The left portion of the stratigraphic chart delineates the stratigraphic code for International Commission on Stratigraphy (Gradstein et al., 2004), the center portion of the stratigraphic chart delineates the regional stratigraphic units (Hentz, 1988), and the right portion of the stratigraphic chart delineates the regional stratigraphic code for the southwestern USA (Gradstein et al., 2004). The regional distribution of stratigraphic units in the study area spans from ~98 to 99° W longitude, 33.5–34° N latitude. Yellow circles denote the sites where pedogenic phyllosilicates and hematites were collected for isotopic analysis and paleotemperature analysis (Table 1). For clarity, the geographic position of the plant sites discussed in this work is not plotted on this map, but given in Table 2. The red dashed lines demarcate the approximate position of stage boundaries for International stratigraphic code (Gradstein et al., 2004) based upon fusilinid (Dunbar and Committee on Stratigraphy, 1960) and conodont (Wardlaw, 2005) biostratigraphy of intercalated marine deposits.

(Savin and Lee, 1988), whereas the oxygen isotope fractionation equation discussed in Yapp (1990) is used for hematite samples (Table 1). Molecular O_2 was evolved from phyllosilicate and hematite samples using BrF_5 reagent that was subsequently converted to CO_2 and analyzed for $\delta^{18}O$ values (Clayton and Mayeda, 1963). Hydrogen isotope compositions of phyllosilicate samples were determined from thermally dehydroxylated (~1000 °C) H_2O that was quantitatively converted to H_2 gas using hot (~760 °C) U-metal (Bigeleisen et al., 1952). Both $\delta^{18}O$ and δD values were measured with a Finnigan MAT 252 Isotope Ratio Mass Spectrometer in the Roy M. Huffington Department of Earth Sciences at Southern Methodist University, and are presented in Table 1. δ values are reported relative to Vienna Standard Mean Ocean Water (VSMOW; Gonfiantini, 1984). Paleotemperature estimates were calculated from the combined $\delta^{18}O$ and δD values of paleosol phyllosilicate minerals (Tabor and Montañez, 2005), which assume isotope equilibrium with meteoric water at the time of mineral crystallization (Delgado and Reyes, 1996; Savin and Hsieh, 1998; Sheldon and Tabor, 2009; Tabor and Montañez, 2005; Yapp, 1993). An independent paleotemperature estimate was calculated by oxygen-isotope-pair-paleothermometry from the $\delta^{18}O$ values of coexisting pedogenic phyllosilicate and hematite (Tabor, 2007), which calculates the temperature required for chemical (i.e., oxygen isotope) equilibrium between coexisting phases.

3.2. Methods for statistical treatment of Paleofloral collections

Plant fossils were excavated from sedimentary detrital siliciclastic strata at 9 localities in the Markley Formation, and from 19 localities in the Archer City and Nocona formations (Table 2). Relative

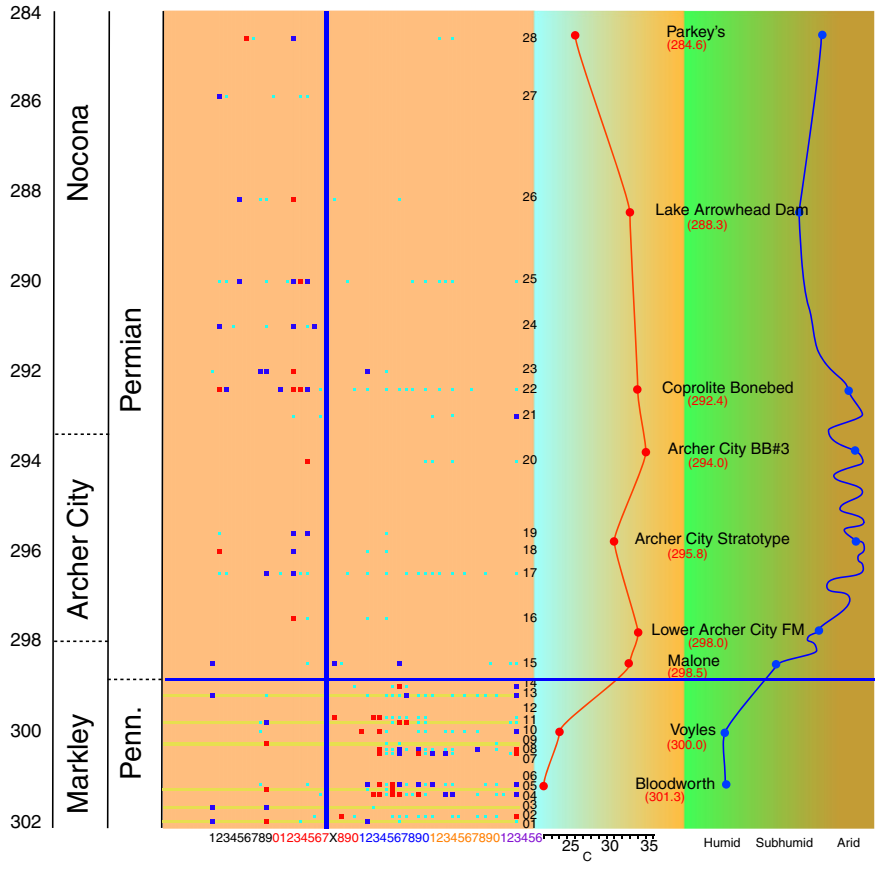

Fig. 2. Floristic, temperature and inferred climatic trends across Pennsylvanian–Permian boundary interval in north-central Texas, USA, plotted using age model employed by (Montañez et al., 2007). Temporal trends in plant distribution shown in the center of the diagram with species abundance indicated by color: Red = abundant (occurs in >50% of sampling quadrats), dark blue = common (in 10–50% of sampling quadrats), and light blue = rare (in <10% of sampling quadrats). Vertical line separates plants typical of high moisture sites (to right of line) from plants of seasonally dry habitats. Numbered left to right, the plants to the left of the line are: *Walchia pinniformis*, *Walchia hypnoides*, *Walchia* cf. *schneideri*, *Walchia* sp., *Walchia* cf. *germanica*, *Brachyphyllum densum*, *Ernestiodendron filiciforme*, Indeterminate conifers, *Sphenopteridium* sp., *Gigantopteridium americanum*, *Russellites* sp., *Taeniopteris jejunata*, *Autunia conferta*, *Rhachiphyllum schenckii*, Cordaitalean leaves, *Odontopteris* sp., and *Mixoneura* spp. Plants to the right of the line are: *Odontopteris lingulata*, *Odontopteris* cf. *brardii*, *Callipteridium* sp., *Eusphenopteris rotundiloba*, *Alethopteris zeilleri*, *Neurodontopteris auriculata*, *Neuropteris ovata*, *Macroneuropteris scheuchzeri*, Indeterminate neuropterids, *Pseudomariopteris cordato-ovata*, calamitalean stems, *Asterophyllites equisetiformis*, *Annularia spicata*, *Annularia carinata*, *Annularia* spp., *Sphenophyllum oblongifolium*, *Sphenophyllum thonii*, *Lilpopia raciborskii*, *Sphenophyllum* spp., *Radstockia* sp., *Dicksonites pluckeneneti*, *Pecopteris plumosa*, *Nemejcopteris feminaeformis*, *Sphenopteris bronnii*, *Sphenopteris* spp., *Oligocarpia* spp., *Discopteris opulenta*, *Daubreeia* sp., Zygopterid foliage, *Sigillaria brardii*, *Danaeites* sp., and *Pecopteris* spp. The twenty-eight sampling sites are numbered from oldest to youngest. 'K' indicates samples from quartz-kaolinite beds: 1—Squaw Mountain K, 2—Turnbow, 3—Turnbow K, 4—Campsey, 5—Cooper K, 6—Cooper, 7—Williamson, 8—Walker, 9—Walker K, 10—Voyles, 11—Markley K, 12—Markley, 13—West Fork Trinity K, 14—West Fork Trinity, 15—Malone, 16—Prideaux, 17—Sanzenbacher, 18—Swinks, 19—Archer City Bone bed, 20—Andrews, 21—Rattlesnake Pasture, 22—Coprolite Bone bed, 23—Copper Mine, 24—Lyles, 25—Thaxton, 26—Rattlesnake Canyon, 27—Black Flat, and 28—Parkey. Plant taxa shown as abundant and common in the lower right quadrant occur in quartz-kaolinite beds (see text) which are stratigraphically intercalated with organic shales and floodplain clastics. Estimated surface air paleotemperatures (red circles) are based on pedogenic phyllosilicate and hematite $\delta^{18}O$ and δD values (Tabor, 2007; Tabor and Montañez, 2005) and inferred paleoclimate (blue circles) are based on paleosol morphological distribution (Tabor and Montañez, 2002; 2004).

Table 1
Stratigraphic position and $\delta^{18}O$ values measured for paleosol hematite and phyllosilicate samples, as well as estimated paleotemperatures based on phyllosilicate–hematite oxygen isotope pair and phyllosilicate δD, $\delta^{18}O$ geothermometry.

Approx. age (Mya)[a]	Stratigraphic age	Formation	Hematite $10^3 \ln^{18}\alpha =$	Hematite $\delta^{18}O$[b]	Phyllosilicate $10^3 \ln^{18}\alpha =$	Phyllo $\delta^{18}O$	T (°C) w/ phyl–hem[c]	T (°C) phyllo δD and $\delta^{18}O$[d]
284.6	Sakmarian	Nocona	–	–	$2.83 * 10^6/T^2 - 5.04$	21.8		26
288.3	Sakmarian	Nocona	–	–	$2.82 * 10^6/T^2 - 5.00$	21.1		33
292.4	Sakmarian	Nocona	–	–	$2.83 * 10^6/T^2 - 5.13$	21.1		34
294.0	Sakmarian	Archer City	$1.63 * 10^6/T^2 - 12.3$	0.5	$2.84 * 10^6/T^2 - 5.08$	20.6	35	35
295.8	Asselian	Archer City			$2.83 * 10^6/T^2 - 4.87$	20.8		31
298.0	Asselian	Archer City	$1.63 * 10^6/T^2 - 12.3$	−0.4	$2.83 * 10^6/T^2 - 5.23$	19.5	37	34
298.5	Asselian	Markley	$1.63 * 10^6/T^2 - 12.3$	−0.1	$2.83 * 10^6/T^2 - 6.20$	19.6	26	33
300.0	Gzhelian	Markley	$1.63 * 10^6/T^2 - 12.3$	0.9	$2.76 * 10^6/T^2 - 6.75$	19.6	24	24
301.3	Gzhelian	Markley	–	–	$2.78 * 10^6/T^2 - 6.11$	20.4	–	22

[a] Approximate ages based on age model developed for north-central Texas study that is reported in Wardlaw (2005) and Montañez et al. (2007).
[b] Calculated end-member hematite $\delta^{18}O$ values reported in Tabor (2007) are also reported here.
[c] Phyllosilicate–hematite oxygen isotope pair paleotemperature estimates from Tabor (2007).
[d] Paired oxygen and hydrogen isotope estimates of paleotemperature from Tabor and Montañez (2005).

abundances of plant taxa, identified either to species or genus level, were assessed quantitatively using the techniques of Pfefferkorn et al. (1975). In this method, all hand samples are treated as sampling quadrats, the presence of a taxon noted only once per quadrat, regardless of how many individual specimens are present. The result is a frequency-of-occurrence for each taxon within the sample suite; hypothetically every taxon could be present on 100% of the quadrats. In practice the resulting taxonomic rank order is comparable to that found with point-count methods (e.g., DiMichele et al., 1991; Lamboy and Lesnikowska, 1988). Frequencies were converted to ranks reflecting percentage occurrence in a sample: 5 = 50–100%, 4 = 10–49%, and 3 = <10%. Specimens occurring one or two times in a sample were noted. All specimens are housed in the Department of Paleobiology, National Museum of Natural History, Washington, DC.

4. Results

4.1. Paleosols

Paleosol morphologies across this transition indicate significant shifts in soil moisture availability, consistent with the temperature rise estimated from the pedogenic minerals hosted by the paleosols (Fig. 2). A shift from the Ultisols and Histosols in the Markley Formation to Aridisols, Vertisols and Alfisols in Permian strata (Tabor and Montañez, 2002, 2004) indicates climatic change from very wet soil conditions with brief periods of seasonal dryness and regionally high water tables to semi-arid and seasonally wet soil conditions with regionally low water tables (DiMichele et al., 2006).

Phyllosilicate $\delta^{18}O$ and δD values (19.5 to 21.8‰; and −68 to −55‰, respectively) and coexisting hematite $\delta^{18}O$ values (−0.2 to 0.9‰) permit estimation of mineral crystallization temperatures during the latest Pennsylvanian through earliest Permian. Phyllosilicate $\delta^{18}O$ and δD values indicate a 13 ± 3 °C increase from a minimum temperature of 22 ± 3 °C during the latest Pennsylvanian and very earliest Permian (Gzhelian to earliest Asselian; Markley Formation) to maximum values of 35 ± 3 °C during the Early Permian (Asselian-Sakmarian; Archer City and Nocona formations; Table 1; Tabor and Montañez, 2005). This significant temperature increase is confirmed by oxygen isotope pairs from coexisting phyllosilicate and hematite, which independently show similar trends from 24 ± 2 °C (latest Pennsylvanian) to 37 ± 3 °C (earliest Permian; Table 1, Fig. 2; Tabor, 2007). The analytically indistinguishable temperature estimates inferred from these two proxies are significant because the results imply that (i) phyllosilicate and hematite crystallized under conditions of chemical equilibrium in the presence of soil moisture that was derived from meteoric water, (ii) they accurately record a significant paleotemperature rise of ~13 ± 3 °C across the Pennsylvanian–Permian boundary, and (iii) the narrow stratigraphic range over which the temperature rise took place implies a relatively rapid transition from cool to warm conditions of mineral crystallization that is commensurate with the fossil floral transition from the hygromorphic- to xeromorphic-dominated biomes.

Table 2
Stratigraphic position and geographic coordinates of the fossil plant sites discussed in this work.

Chart #	Location (Loc.) name	USNM Loc. #s	Latitude	Longitude
1	Parkey's Oil Patch	38896	33° 35′ 00″ N	99° 00′ 00″ W
2	South of Black Flats	40019; 40021	33° 40′ 00″ N	98° 50′ 00″ W
3	Rattlesnake Canyon	40065	33° 40′ 00″ N	98° 50′ 00″ W
4	Thaxton	40037	33° 50′ 00″ N	98° 05′ 00″ W
5	Lyles	40030	33° 40′ 00″ N	98° 45′ 00″ W
6	Copper Mine	40026; 40074	33° 40′ 00″ N	98° 40′ 00″ W
7	Coprolite Bone Bed	40027; 40028; 40029	33° 40′ 00″ N	99° 40′ 00″ W
8	Rattlesnake Pasture	40637; 40638	33° 30′ 00″ N	98° 30′ 00″ W
9	Andrews	40031	33° 25′ 00″ N	98° 35′ 00″ W
10	Archer City Bone Bed	40025	33° 35′ 00″ N	98° 40′ 00″ W
11	Swinks	40631	33° 20′ 00″ N	99° 00′ 00″ W
12	Sanzenbacher	40986; 40600	33° 40′ 00″ N	98° 00′ 00″ W
13	Prideaux Ironstones	40634	33° 25′ 00″ N	98° 30′ 00″ W
14	Malone	42135	33° 30′ 00″ N	98° 25′ 00″ W
15	281 Road Cut	40079; 40080; 40596	33° 35′ 00″ N	99° 00′ 00″ W
	281 Road Cut	40633	33° 35′ 00″ N	99° 00′ 00″ W
17	North of Markley	40693	33° 25′ 00″ N	98° 25′ 00″ W
18	North of Markley	40064	33° 25′ 00″ N	98° 25′ 00″ W
19	Voyles	39989; 39994	33° 25′ 00″ N	98° 20′ 00″ W
20	Walker	40087; 40088; 40595	33° 25′ 00″ N	98° 05′ 00″ W
21	Walker	40007	33° 25′ 00″ N	98° 05′ 00″ W
22	Williamson Drive	40012; 40013	33° 25′ 00″ N	98° 10′ 00″ W
23	Cooper	40068; 40000	33° 25′ 00″ N	98° 10′ 00″ W
24	Cooper	39992	33° 25′ 00″ N	98° 10′ 00″ W
25	Bloodworth	40693; 40004	33° 25′ 00″ N	98° 10′00″ W
26	Turnbow	39998	33° 30′ 00″ N	97° 50′ 00″ W
27	Turnbow	39997	33° 30′ 00″ N	97° 50′ 00″ W
28	Squaw Mountain	39990; 40002	33° 20′ 00″ N	98° 20′ 00″ W

Blue — no real significance other than to set it off as the heading row.
Orange — Permian.
Yellow and Red — Pennsylvanian.
Yellow — wetland floras.
Red — seasonally dry floras.

4.2. Fossil floras

Strongly directional vegetational changes are closely correlated with the temperature and soil moisture changes (see Table 2, Fig. 2) through the study section. Markley Formation (Gzhelian to earliest Asselian) floras are typical of Late Pennsylvanian tropical wetlands, consisting of arborescent medullosan pteridosperms, tree ferns, calamitalean sphenopsids, and sigillarian lycopsids, and ground cover that included pteridosperms, ferns, and sphenopsids (Table 2; summary of Markley flora: DiMichele et al., 2005; Tabor et al., in press). In uppermost Pennsylvanian deposits, below the stratigraphic interval recording the temperature increase, xeromorphic plants, dominantly conifers and *Sphenopteridium*, are preserved in thin quartz-rich kaolinite beds intercalated within sequences of paleosols, organic shales/coals, and flood-plain derived siliciclastics containing the typical Late Pennsylvanian wetland flora (DiMichele et al., 2005; Tabor et al., in press). Although the wetland and seasonally-dry biomes may occur together at any given outcrop, they are mutually exclusive in terms of the beds in which they occur, and in taxonomic composition. The <40 m thick transitional interval recording the temperature rise contains a mixed flora including conifers, medullosan pteridosperms (*Odontopteris*), and calamites (Table 2, Fig. 2). Successively younger Early Permian floras are increasingly dominated by arborescent xeromorphic plants (Table 2; Fig. 2; see Labandeira and Allen, 2007, for a comprehensive description of a typical Nocona Formation flora), although some typically Pennsylvanian ground cover plants persist into the Early Permian. Ground cover has low transport potential and tends to be drawn from sites near the depositional environment, possibly stream sides, where wet conditions would have been most persistent (Burnham, 1989; Scheihing, 1980). Tree ferns, which occur sporadically in the Early Permian, also may have grown under such conditions (DiMichele et al., 2006).

The floral changes between the coal-bearing Late Pennsylvanian (Gzhelian; Markley Formation) and non-coal-bearing earliest Permian (Asselian–Sakmarian; uppermost Markley, Archer City, Nocona formations) are dramatic. Plants from landscapes with high moisture availability, mainly sphenopsids and tree ferns, become rare in Permian strata. The former are characteristic of aggradational environments — watercourses and lake margins (Gastaldo, 1992); the latter are opportunistic "weeds" that occur sporadically through the Early Permian associated with landscape "wet spots" or pluvial intervals (DiMichele et al., 2006). The "wet" flora is replaced by one dominated by conifers, callipterids, and taeniopterids (cf. Kerp and Haubold, 1988). A considerable reduction in complexity of plant-bearing outcrops accompanies this

vegetational change. Plant-bearing outcrops of the latest Pennsylvanian Markley Formation consist of several different lithologies, each with a distinct flora. In contrast, plant-bearing Early Permian outcrops of the uppermost Markley, Archer City and Nocona formations are monolithic, with a single flora confined to homogenous red or gray mudstone-filled channels. The "Permian"-type xeromorphic flora found in thin beds within the Markley Formation becomes dominant in the Archer City Formation following the temperature increase. Thus, the seasonally dry flora was present on the landscape during earlier times but was confined to peripheral, moisture-limited habitats most of the time, moving into the basin periodically. Lowland drying, which accompanied the temperature increase, facilitated the permanent residence of this "Permian" flora in the basinal lowlands.

5. Discussion and conclusions

5.1. Putting isotope-based paleotemperature estimates into context

The similarity between paleotemperature estimates from single-mineral-based oxygen and hydrogen isotope compositions of phyllosilicates and oxygen isotope mineral-pair-based estimates of co-existing phyllosilicate and hematite in Permo-Carboniferous paleosol profiles from north-central Texas is a persuasive evidence that these minerals crystallized (i) under equilibrium conditions in the soil, (ii) in the presence of meteoric water that had not been substantially altered by other processes such as evaporation and that (iii) these temperature estimates are credible representatives of actual Permo-Carboniferous soil temperatures. Yet, it is unclear how these soil temperature estimates correspond to surface air temperatures. Temperature records in modern soils have consistently shown that soil temperatures at 50 cm depth are typically 1 to 2 °C warmer than those of mean surface air temperatures (e.g., Buol et al., 1997). Furthermore, recent work with isotopologues ($^{47}\Delta$) from pedogenic calcite in modern soils indicates that particular temperature proxy consistently crystallizes at soil temperatures well above that of mean annual surface air temperatures (Passey et al., 2010; Quade et al., 2012) and typically provides estimates close to the mean warm-season surface air temperature (Passey et al., 2010).

In order to gain some perspective on the meaning of the Permo-Carboniferous soil paleotemperature estimates and explain their relationship to surface air paleotemperatures in a more comprehensive way, we consider soil- and surface-air temperatures from modern tropical and paratropical sites that, though not exact analogs, permit us to compare the ancient tropics to those of the modern Earth. Mineral crystallization temperature estimates were calculated from analyses of samples that were collected from between 30 and 60 cm beneath the interpreted paleo-surface of the Pennsylvanian–Permian paleosol profiles. In addition, these paleosols developed in low-altitude tropical environments (~0–5° N) on a continent affected at least intermittently by monsoonal precipitation patterns (Parrish, 1993; Tabor and Montañez, 2002). Therefore, we will limit our comparison of modern soil- and surface-air temperatures to low-altitude (<200 m above sea level) tropical African sites between latitudes 10° N and 10° S because this region also is affected by seasonal and monsoonal precipitation. This results in observations of monthly mean annual cycles of soil- and surface-air temperatures among 31 sites (Table 3; Chang, 1958) from Angola, Ivory Coast, Ghana, Guinea and Nigeria.

These 31 sites include a mean annual surface air temperature range of ~24–29 °C (Fig. 3), mean annual precipitation range of 32–378 cm, rainy days (a minimum estimate of cloud cover and direct solar heating) range of 18–187, and mean humidity range of 35–90% (Table 3). Furthermore, soil temperature measurements among these sites were taken from tropical dry forest, tropical wet forest, and savanna ecosystems. Mean annual soil temperature between 30 and 60 cm depths exceeds its corresponding mean annual surface air temperature at each site by 0.3–5.0 °C (Fig. 3; Table 3). Furthermore, seasonal

Table 3
Modern soil- and surface-air temperatures from tropical Africa.

Location	Latitude	Longitude	Soil temp (°C)	Soil temp 1σ (°C)	Surface air temp (°C)	Soil temp–air temp	Mean annual precipitation	Rainy days	Altitude (masl)
Cabinda, Angola	5°33′ S	12°11′ E	27.9	1.5	25.0	2.9	67	51	20
Luanda, Angola	8°49′ S	13°13′ E	29.4	2.2	24.4	5.0	33	26	42
Onga Zanga, Angola	9°7′ S	13°42′ E	28.1	1.2	24.4	3.7	33	26	43
Abidjan, Ivory Coast	5°15′ N	3°56′ W	29.9	1.4	25.0	4.9	194		75
Conakry, Guinea	9°34′ N	13°37′ W	29.6	1.8	26.4	3.2	378	129	22
Lome Ivory Coast	6°10′N	1°15′ E	30.4	1.2	25.0	5.4	194		26
Tabou, Ivory Coast	4°25′ N	7°22′ W	29.0	1.6	26.1	2.9	228	148	22
Zinder, Ivory Coast	4°25′ N	7°22′ W	30.6	3.1	26.1	4.5	228	148	0
Accra, Ghana	5°36′ N	0°10′ W	30.2	1.3	26.8	3.4	73	54	59
Aiyinasi, Ghana	5°2′ N	2°28′ W	27.1	1.1	26.7	0.4		47	41
Asuansi, Ghana	5°2′ N	1°15′ W	27.8	1.4	26.7	1.1		33	104
Kpeve, Ghana	6°42′ N	0°20′ E	28.3	0.8	26.9	1.4	137		152
Kumasi, Ghana	5°36′ N	0°10′ W	28.4	1.5	25.6	2.8	140	51	59
Kwadaso, Ghana	6°42′ N	1°39′ W	27.6	0.9	25.6	2.0	140	51	244
Nungwa, Ghana	5°41′ N	0°6′ W	28.4	1.1	27.2	1.2	79	45	30
Odumase Krobo, Ghana	6°7′ N	0°0′ W	28.5	1.1	28.3	0.2	114	25	70
Pokuase, Ghana	5°40′ N	0°16′ W	28.6	1.2	27.2	1.4	105		50
Takoradi, Ghana	4°53′ N	1°46′ W	28.7	1.3	26.7	2.0	120	57	5
Tamale, Ghana	9°25′ N	0°53′ W	30.7	2.5	28.9	1.8	109	28	182
Badeggi, Nigeria	9°45′ N	6°7′ E	29.8	1.3	28.9	0.9	30	19	118
Barombi-Kang, Nigeria	4°35′ N	9°26′ E	27.4	0.4	25.7	1.7	247	187	182
Benin, Nigeria	6°33′ N	5°37′ E	27.1	1.3	26.7	0.4	193	57	145
Ikeja, Nigeria	6°35′ N	3°20′ E	28.7	1.0	27.2	1.5	154	53	39
Irrua, Nigeria	6°44′ N	6°13′ E	27.5	1.5	26.7	0.8	64		182
Makurdi, Nigeria	7°41′ N	8°37′ E	29.2	1.1	27.8	1.4	20	25	96.1
Mokwa, Nigeria	9°19′ N	5°2′ E	29.8	2.3	28.9	0.9	32	18	152
Nkwelle, Nigeria	6°14′ N	6°50′ E	28.3	1.3	27.0	1.3	31		91
Obio Akpa, Abak, Nigeria	4°59′ N	7°47′ E	27.0	0.8	26.7	0.3	296		58
Oyo Stock Farm, Nigeria	7°54′ N	3°43′ E	31.7	1.4	26.7	5.0	54	38	61
Port Harcourt, Nigeria	4°51′ N	7°1′ E	27.3	0.7	26.7	0.6	229	67	20
Umudike, Nigeria	5°29′ N	7°33′ E	28.2	1.3	26.1	2.1	79		121
Yandev, Nigeria	7°23′ N	9°1′ E	29.2	1.5	24.7	4.5	106	25	121

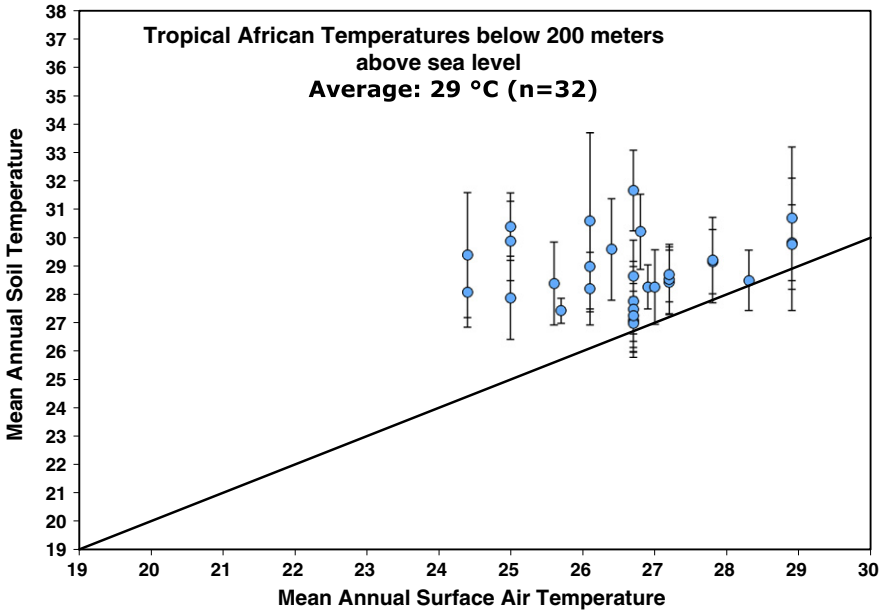

Fig. 3. Plot of mean annual soil temperatures between 30 and 60 cm depth in the soil vs. corresponding mean annual surface air temperatures recorded from modern sites in equatorial Africa (Table 3; Chang, 1958). Y-axis error bars correspond to seasonal variance (1σ) of soil temperatures around the mean annual temperature in the soil. See text for discussion.

variance of soil temperature ranges from 0.4 to 3.1 °C; this is far less of a seasonal range than is encountered in the subtropics and midlatitudes (e.g., Quade et al., 2012) and arid tropics (Passey et al., 2010) based on clumped isotope proxy data from calcareous soils (note, however, that many soils in equatorial Africa do commonly contain carbonate, e.g., Acquaye et al., 1990). It is unclear which factor(s) is responsible for (1) how much warmer a mean annual soil temperature is with respect to its corresponding mean annual surface air temperature or (2) the magnitude of seasonal variation of soil temperature. Neither variable shows correlation with precipitation amount, number of rainy days, mean humidity, location or ecosystem. Yet, the average temperature of these tropical soils is 2.1 ± 1.6 °C (1σ) warmer than the average surface air temperature. Therefore, it is likely that tropical soil minerals will have stable oxygen and hydrogen isotopic compositions that record temperatures of crystallization that are ~2 °C warmer than surface air temperatures.

Among the 31 modern sites in tropical Africa, soil temperatures between 30 and 60 cm depth average 28.8 ± 1.2 °C (1σ; Fig. 3; Table 3). Most of the Permian (Asselian, Sakmarian) soil temperature estimates are analytically indistinguishable from the range of soil temperatures observed in modern tropical Africa (Tables 1, 3; Figs. 2, 3). This comparison of Permo-Carboniferous soil temperature estimates to modern tropical soil temperatures in Africa suggests that the Late Pennsylvanian tropics were at times substantially *cooler* than the modern tropics by perhaps up to 6 °C. Remarkably, it is the Pennsylvanian (Gzhelian) soil temperature estimates from the Markley Formation that have no analogs in modern tropical Africa (at low altitudes).

5.2. Onset of "big ice"

The Pennsylvanian–Permian transition interval has been identified as a period of major ice expansion in the southern hemisphere. It has been argued that this expansion should have, and did have, a major effect on sea-level (Rygel et al., 2008) and left a mark in areas such as carbonate platforms, which would be expected to be sensitive to a major change in sea level (Koch and Frank, 2011). The absence of a clear lithological indication of this change in the terrestrial Markley Formation is, perhaps, not particularly worrisome, given the large number of hiatuses, marked by paleosols, in this, as in any other largely terrestrial sections. A considerable amount of time is represented by paleosol surfaces. However, the evidence for significant changes in temperature and marked vegetational changes is consistent with some kind of major environmental change.

The absence of a clear hiatus at the Pennsylvanian–Permian boundary is seen in other terrestrial sections from Western Europe (Roscher and Schneider, 2006), through the Dunkard Group in the Appalachians (Fedorko and Skema, 2011; Martin, 1998), to the southwestern United States (Condon, 1997). In mixed terrestrial-marine sections, such as in the Midcontinent United States (Sawin et al., 2006), there is evidence of continuous cyclothemic deposition across the boundary, again not indicative of a major physical hiatus (Olszewski and Patzkowsky, 2003; Mazzullo et al., 2007). In New Mexico, there are numerous hiatuses within the transitional interval, yet none stands out at least as presently described, as of particular note (e.g., Krainer and Lucas, 2010; Lucas and Krainer, 2004). Yet in all of these basins, there is some evidence of significant vegetational change near the boundary (DiMichele and Chaney, 2005; Kerp and Fichter, 1985; Lupia, 2010; White, 1936; Wilson and Rashid, 1975).

Observations from Permo-Carboniferous tropical and subtropical carbonate platforms indicate a basinward facies shift very near the Pennsylvanian–Permian boundary that is interpreted to represent development of large-scale continental ice-building in Gondwanaland (Koch and Frank, 2011). The stratigraphic record above this supposed ice-building event is composed of cyclic marine or mixed-marine and continental strata interpreted to represent 4th or 5th order depositional cycles through the Asselian–Sakmarian (Koch and Frank, 2011). As mentioned, the age of strata in the eastern Midland basin of north-central Texas is not known with precision. Because of this it is tempting to attribute the very low tropical soil temperature estimates from the Markley Formation to the interval of ice-building ("Big Ice") near the Pennsylvanian–Permian boundary, a hypothesis supported by a long-lived and stepped offlap in the Donets Basin, interpreted to be a large magnitude lowstand that was initiated in the latest Pennsylvanian (latter half of the Gzhelian) (Eros et al., 2012). Future work will seek to document the timing and duration of this tropical "cool" phase in the Midland basin as well as other tropical basins.

Our conclusion from these observations is that the north-central Texas pattern is consistent with a major environmental change that affected large parts of equatorial Pangea. These changes may have begun slightly earlier in the western reaches of the equatorial region, where

climates were generally more seasonally dry, even during the most intensely wet portions of any given glacial–interglacial cycle. There were early and abundant occurrences of conifers and other elements of the seasonally dry flora in the Pennsylvanian of western Pangea (Falcon-Lang et al., 2011), but their rise to landscape dominance in basinal lowlands, and the constriction and biodiversity collapse of the wetland biota, clearly accelerated across the Pennsylvanian–Permian geological transition.

5.3. Implications for modern and future tropics

A modern parallel to the Pennsylvanian–Permian floral change pattern exists in Quaternary Amazonia (Colinvaux et al., 1996; Jaramillo et al., 2006; Jipp et al., 1998), where a few high-altitude taxa, particularly the conifer *Podocarpus*, appear in low altitude tropical rainforests during glacial maxima. In this case, the incumbent vegetation remained intact but accommodated brief invasions of allochthonous elements, driven by cooling temperatures. The Pleistocene glacial–interglacial climate modes resulted in tropical temperature variations of ~3° to 5 °C (Ziegler et al., 1997), and the concomitant tropical floral transitions across them were significant. Such floral shifts, however, pale in comparison to the temperature and floristic changes of the late Paleozoic, which were of a larger magnitude and lead to collapse of the wet biome and extirpation of most of its species pool throughout western and central Pangea (DiMichele et al., 1996; Falcon-Lang and DiMichele, 2010). The physical region of the tropics, under the changed climatic regime, was filled by species of the previously poorly represented, low diversity seasonally-dry to xeric biome. Wet biome elements were reduced to a small subset, represented by weedy tree ferns or riparian specialists.

It is possible that regional climatic drying alone led to the deterioration of the wet biome and, at the same time, resulted in improved drainage of soils, which decreased the heat capacity of soil materials and reduced shade cover over the landscape that led to the apparent 13 ± 3 °C increase in soil mineral crystallization temperatures. Nevertheless, the temperature increase documented here corresponds to sensible heat and therefore would have existed as an additional stress on floras in the region. For each month with a mean temperature above 0 °C, potential evapotranspiration of soil moisture is about 0.2 mm/°C/day (Oliver, 1987) in modern ecosystems. A temperature change from 22° ± 3 °C to 35° ± 3 °C corresponds to a doubling of annual potential evapotranspiration from 1387–1825 mm to 2336–2775 mm, an effective increase in potential soil-moisture loss of up to ~60%. Note that this corresponds to potential evapotranspiration, and probably does not accurately depict the actual amount of water lost from the soil profiles through evapotranspiration. Rather, we consider the actual evaporation to have been relatively low during the Pennsylvanian "cool" mode in the Markley Formation that is associated with the dominance of the hygromorphic plant biome that experienced minimal water stress. Actual evaporation increased during the transition from the hygromorphic to xeromorphic plant biome in response to rising temperatures and the availability of moisture on the landscape (as evidenced by gleyed and plinthic paleosol morphologies in the transitional stratigraphy; DiMichele et al., 2006; Tabor and Montañez, 2004; Tabor et al., in press). Because of overall drier conditions in the Early Permian, actual evapotranspiration was relatively low as the water-stress tolerant xeromorphic biome rose to dominance.

It is significant that the period of vegetational change is stratigraphically short compared to the range of stable conditions for the hygromorphic- and xeromorphic-dominated biomes and therefore implies that the transition corresponds to a relatively rapid geological event. However, and more importantly, the flora appears to have been resistant to change during the initial phases of the temperature rise (Fig. 2). During this interval, taxonomic richness of the wetland flora declined but it continued to dominate the lowland basinal landscape. The exact temporal duration during which this declining flora continued to hold sway cannot be determined from our data. It is clear, however, that the lag was short compared to the length of the transitional interval and to the length of time that the subsequent xeric vegetation persisted in the lowland depositional basins. This lag may be analogous to "vegetational inertia" (Cole, 1985) recognized in Pleistocene pluvial–interpluvial transitions in the southwestern USA. And it suggests a threshold-like response to directionally changing environmental conditions (DiMichele et al., 2009).

The coupled Pennsylvanian–Permian climate-floral reconstruction presented here indicates that continued continental warming and the associated hydrological changes could bring on rapid, and effectively irreversible, regional ecological changes. Using these late Paleozoic patterns as a model, such ecological change could be accompanied by increased species pool fragmentation, consequent biogeographic heterogeneity of the tropics, and a general trend toward increased abundance of plants with tolerance to environmental fluctuations, particularly tolerance to periods of moisture deficits. The Paleozoic data also suggest that the change from spatial dominance of one vegetation type to dominance of an entirely different type could occur in a threshold-like manner, with little easily interpretable warning signs of approach to a threshold point.

Acknowledgments

WD and DSC acknowledge the NMNH small grants program and the Smithsonian Institution Scholarly Studies program for research support, particularly of north-central Texas fieldwork. We thank numerous property owners for granting access to their land during the period from 1989 until the present, during which this study has been carried out. NJT was funded by NSF-EAR 0844147 and NSF-EAR 0519336.

References

Acquaye, D.K., Dowuona, G.N., Mermut, A.R., St. Arnaud, R.J., 1990. Micromorphology and mineralogy of cracking soils in the Accra Plains of Ghana. Soil Science Society of America 56, 193–201.
Bigeleisen, J., Perlman, M.L., Prosser, H.C., 1952. Conversion of hydrogenic materials to hydrogen for isotopic analysis. Analytical Chemistry 34, 1356–1357.
Boyce, C.K., Lee, J.-E., Field, T.S., Brodribb, T.J., Zwieniecki, M.A., 2010. Angiosperms helped put the rain in the rainforests: the impact of plant physiological evolution on tropical biodiversity. Annals of the Missouri Botanical Garden 527–540. http://dx.doi.org/10.3417/2009143 (12/2010).
Broutin, J., Doubinger, J., Farjanel, G., Freytet, P., Kerp, H., 1990. Le renouvellement des flores au passage Carbonifère Permien: approches stratigraphiques, biologiques, sédimentologiques. Comptes Rendus Académie des Sciences 321, 1563–1569.
Buol, S.W., Hole, F.D., McCracken, R.J., Southard, R.J., 1997. Soil Genesis and Classification, 4th ed. Iowa State University Press, Ames, Iowa (527 pp.).
Buol, S.W., Southard, R.J., Graham, R.C., McDaniel, P.A., 2003. Soil Genesis and Classification, 5th ed. Iowa State Press, Ames, Iowa, USA, (494 p).
Burnham, R.J., 1989. Relationships between standing vegetation and leaf litter in a paratropical forest: implications for paleobotany. Review of Palaeobotany and Palynology 58, 5–32.
Bush, M.B., Gosling, W.D., Collinvaux, P.A., 2007. Climate and vegetation change in the lowlands of the Amazon Basin. In: Bush, M.B., Flenley, J.R. (Eds.), Tropical Rainforest Responses to Climate Change. Praxis, Chichester, pp. 61–84.
Chang, J., 1958. Ground Temperatures, vol. 2. Harvard University Press (196 pp.).
Clayton, R.N., Mayeda, T.K., 1963. The use of bromine pentafluoride in the extraction of oxygen from oxides and silicates for isotopic analysis. Geochimica et Cosmochimica Acta 27, 43–52.
Cole, K., 1985. Past rates of change, species richness, and a model of vegetational inertia in the Grand Canyon, Arizona. The American Naturalist 125, 289–303.
Colinvaux, P.A., de Oliveira, P.E., Moreno, J.E., Miller, M.C., Bush, M.B., 1996. A long pollen record from lowland Amazonia: forest and cooling in glacial times. Science 274, 85–88.
Condon, S.B., 1997. Geology of the Pennsylvanian and Permian Cutler Group and Permian Kaibab limestone in the Paradox Basin, southeastern Utah and southwestern Colorado. U.S. Geological Survey Bulletin 2000-P (1–46).
Delgado, A., Reyes, E., 1996. Oxygen and hydrogen isotope compositions in clay minerals: a potential single-mineral geothermometer. Geochimica et Cosmochimica Acta 60, 4285–4289.
DiMichele, W.A., Philips, T.L., McBrinn, G.E., 1991. Quantitative analysis and paleoecology of the Secor coal and roof shale floras (Middle Pennsylvanian, Oklahoma). Palaios 6, 390–409.
DiMichele, W.A., Aronson, R.B., 1992. The Pennsylvanian–Permian vegetational transition: a terrestrial analogue to the onshore-offshore hypothesis. Evolution 46, 807–824.

DiMichele, W.A., Chaney, D.S., 2005. Pennsylvanian–Permian fossil floras from the Cutler Group, Cañon del Cobre and Arroyo del Agua areas in northern New Mexico. New Mexico Museum of Natural History and Science Bulletin 31, 26–33.
DiMichele, W.A., Pfefferkorn, H.W., Phillips, T.L., 1996. Persistence of Late Carboniferous tropical vegetation during glacially driven climatic and sea-level fluctuations. Palaeogeography, Palaeoclimatology, Palaeoecology 125, 105–128.
DiMichele, W.A., Tabor, N.J., Chaney, D.S., 2005. Outcrop-scale environmental heterogeneity and vegetational complexity in the Permo-Carboniferous Markley Formation of North Central Texas. In: Lucas, S.G., Zeigler, K.E. (Eds.), The Nonmarine Permian. New Mexico Museum of Natural History and Science Bulletin, 30, pp. 60–66.
DiMichele, W.A., Tabor, N.J., Chaney, D.S., Nelson, W.J., 2006. From wetlands to wet spots: environmental tracking and the fate of Carboniferous elements in Early Permian tropical floras. In: Greb, S.F., DiMichele, W.A. (Eds.), Wetlands Through Time. Geological Society of America Special Paper, 399, pp. 223–248.
DiMichele, W.D., Montañez, I.P., Poulsen, C.J., Tabor, N.J., 2009. Feedbacks and regime shifts in the Late Palaezoic ice-age Earth. Geobiology 7, 200–226.
DiMichele, W.A., Kerp, H., Sirmons, R., Fedorko, N., Skema, V., Blake Jr., B.M., Cecil, C.B., 2013. Callipterid peltasperms of the Dunkard Group, Central Appalachian Basin. International Journal of Coal Geology 119, 56–78.
Dunbar, C.O., Committee on Stratigraphy, 1960. Correlation of the Permian formations of North America. Geological Society of America Bulletin 71, 1763–1806.
Eble, C.F., Grady, W.C., Blake, B.M., 2013. Dunkard Group coal beds: palynology, coal petrography and geochemistry. International Journal of Coal Geology 119, 32–40.
Eros, J.M., Montañez, I.P., Osleger, D.A., Davydov, V.I., Nemyrovska, T., Poletaev, V., Zhykalyak, M.V., 2012. Sequence stratigraphy and onlap history, Donets Basin, Ukraine: insight into Late Paleozoic ice age dynamics. Palaeogeography. Palaeoclimatology. Palaeoecolecology 313–314, 1–25.
Falcon-Lang, H.J., DiMichele, W.A., 2010. What happened to the coal forests during Pennsylvanian glacial phases? Palaios 25, 611–617.
Falcon-Lang, H.J., Jud, N.A., Nelson, W.J., DiMichele, W.A., Chaney, D.S., Lucas, S.G., 2011. Pennsylvanian coniferopsid forests in sabkha facies reveal the nature of seasonal tropical biome. Geology 39, 371–375.
Fedorko, N., Skema, V., 2011. Stratigraphy of the Dunkard Group in West Virginia and Pennsylvania. In: Harper, J.A. (Ed.), Geology of the Pennsylvanian–Permian in the Dunkard Basin. Guidebook, 76th Annual Field Conference of Pennsylvania Geologists, Washington, PA, pp. 1–25.
Fielding, C.R., Frank, T.D., Isbell, J.L., 2008. The late Paleozoic ice age—a review of current understanding and synthesis of global climate patterns. In: Fielding, C.R., Frank, T.D., Isbell, J.L. (Eds.), Resolving the Late Paleozoic Ice Age in Time and Space. Geological Society of America Special Paper, 441, pp. 343–354.
Gastaldo, R.A., 1992. Regenerative growth of fossil horsetails following burial by alluvium. Historical Biology 6, 203–219.
Gastaldo, R.A., DiMichele, W.A., Pfefferkorn, H.W., 1996. Out of the icehouse into the greenhouse: a late Paleozoic analogue for modern global vegetational change. GSA Today 6, 1–7.
Giral-Kacmarcik, S., Savin, S.M., Nahon, D.B., Girard, J.P., Lucas, Y., Abel, L.J., 1998. Oxygen isotope geochemistry of kaolinite in laterite-forming processes, Manaus, Amazonas, Brazil. Geochimica et Cosmochimica Acta 62, 1865–1879.
Gonfiantini, R., 1984. Advisory group meeting on stable isotope reference samples for geochemical and hydrological investigations. Report to the Director General. Vienna, Austria (77 p).
Gradstein, F., Ogg, J., Smith, A., 2004. A Geologic Time Scale 2004. Cambridge University Press, Cambridge, U.K. (589 p).
Hentz, T.F., 1988. Lithostratigraphy and paleoenvironments of upper Paleozoic continental red beds, north-central Texas: Bowie (new) and Wichita (revised) Groups. Bureau of Economic Geology Report of Investigations 170, 49 p.
Hentz, T.F., Brown Jr., L.F., 1987. Wichita Falls-Lawton Sheet. In: Barnes, V.E. (project director), Geologic Atlas of Texas: The University of Texas at Austin, Bureau of Economic Geology, Scale 1:250,000.
Isbell, J.L., Miller, M.F., Wolfe, K.L., Lenaker, P.A., 2003. Timing of late Paleozoic glaciation in Gondwana: was glaciation responsible for the development of northern hemisphere cyclothems? In: Chan, M.A., Archer, A.W. (Eds.), Extreme Depositional Environments: Mega End Members in Geologic Time, Geological Society of America Special Paper, 370, pp. 5–24.
Isbell, J.L., Henry, L.C., Gulbranson, E.L., Limarino, C.O., Fraiser, M.L., Koch, Z.J., Ciccioli, P.L., Dineen, A.A., 2012. Glacial paradoxes during the late Paleozoic ice age: evaluating the equilibrium line altitude as a control on glaciation. Gondwana Research 22, 1–19.
Jaramillo, C., Rueda, M.J., Mora, G., 2006. Cenozoic plant diversity in the neotropics. Science 311, 1893–1896.
Jipp, P.H., Nepstad, D.C., Cassek, D.K., De Carvalho, C.R., 1998. Deep soil moisture and transpiration in forests and pastures of seasonally-dry Amazonia. Climatic Change 39, 395–412.
Kerp, H., 1996. Post-Variscan late Palaeozoic Northern Hemisphere gymnosperms: the onset to the Mesozoic. Review of Palaeobotany and Palynology 90, 263–285.
Kerp, H., Fichter, J., 1985. Die Makrofloren des saarpfälzischen Rotliegenden (? Ober-Karbon – Unter-Perm; SW-Deutschland). Mainzer Geowissenschaftliche Mitteilungen 14, 159–286.
Kerp, H., Haubold, H., 1988. Aspects of Permian palaeobotany and palynology. VIII. On the reclassification of the West- and central European species of the form-genus *Callipteris* Brongniart 1849. Review of Palaeobotany and Palynology 54, 135–150.
Koch, J.T., Frank, T.D., 2011. The Pennsylvanian–Permian transition in the low-latitude carbonate record and the onset of major Gondwanan glaciation. Palaeogeography, Palaeoclimatology, Palaeoecology 308, 362–372.
Krainer, K., Lucas, S.G., 2010. Sedimentology of the Pennsylvanian–Permian Cutler Group and Lower Permian Abo Formation, northern New Mexico. New Mexico Museum of Natural History and Science Bulletin 49, 25–36.
Labandeira, C.C., Allen, E.G., 2007. Minimal insect herbivory for the Lower Permian Coprolite Bone Bed site of north-central Texas, USA, and comparison to other Late Paleozoic floras. Palaeogeography, Palaeoclimatology, Palaeoecology 247, 197–219.
Lamboy, W., Lesnikowska, A., 1988. Some statistical methods useful in the Analysis of plant paleoecological data. Palaios 3, 86–94.
Lucas, S.G., 2006. Global Permian tetrapod biostratigraphy and biochronology. In: Lucas, S.G., Cassinis, G., Schneider, J.W. (Eds.), Non-Marine Permian Biostratigraphy and Biochronology. Geological Society of London Special Publications, pp. 65–93.
Lucas, S.G., Krainer, K., 2004. The Red Tanks Member of the Bursum Formation in the Lucero Uplift and regional stratigraphy of the Bursum Formation in New Mexico. New Mexico Museum of Natural History and Science Bulletin 25, 43–52.
Lupia, R., 2010. Palynology of the Pennsylvanian–Permian transition, Wood Siding (Virgilian) to Wellington (Leonardian) Formations, in North-Central Oklahoma. Geological Society of America Abstracts with Programs 42 (5), 193.
Martin, W.D., 1998. Geology of the Dunkard Group (Upper Pennsylvanian–Lower Permian) in Ohio, West Virginia, and Pennsylvania. Ohio Geological Survey Bulletin 73, 1–49.
Mazzullo, S.J., Boardman, D.R., Grossman, E.L., Dominick-Wells, K., 2007. Oxygen-carbon isotope stratigraphy of Upper Carboniferous to Lower Permian marine deposits in midcontinent U.S.A. (Kansas and NE Oklahoma): implications for seawater chemistry and depositional cyclicity. Carbonates and Evaporites 22, 55–72.
McInerney, F.A., Wing, S.L., 2011. The Paleocene–Eocene Thermal Maximum: a perturbation of carbon cycle, climate, and biosphere with implications for the future. Annual Review of Earth and Planetary Sciences 39, 489–516.
Montañez, I.P., Poulsen, C.J., 2013. The Late Paleozoic Ice Age: an evolving paradigm. Annual Reviews in Earth and Planetary Sciences 41, 24.1–24.28.
Montañez, I.P., Tabor, N.J., Niemeier, D., DiMichele, W.A., Frank, T.D., Fielding, C.R., Isbell, J.L., 2007. CO_2-forced climate and vegetation instability during Late Paleozoic deglaciation. Science 315, 87–91.
Nelson, W.J., Hook, R.W., Tabor, N., 2001. Clear Fork Group (Leonardian, Lower Permian) of North-Central Texas. Oklahoma Geological Survey Circular 104, 167–169.
Oliver, J.E., 1987. Evapotranspiration. In: Oliver, J.E., Fairbridge, R.W. (Eds.), The Encyclopedia of Climatology. Van Nostrand Reinhold, New York, pp. 449–456.
Olszewski, T.D., Patzkowsky, M.E., 2003. From cyclothems to sequences: the record of eustasy and climate on an icehouse epeiric platform (Pennsylvanian–Permian, North American midcontinent). Journal of Sedimentary Research 73, 15–30.
Opluštil, S., 2013. Flora from the Líně Formation (Czech Republic) as an example of floristic dynamics around the Carboniferous/Permian boundary. New Mexico Museum of Natural History and Science Bulletin 60, 314–321.
Parrish, J.T., 1993. Climate of the supercontinent Pangea. Journal of Geology 101, 215–233.
Passey, B.H., Levin, N.E., Cerling, T.E., Brown, F.H., Eiler, J.M., 2010. High-temperature environments of human evolution in East Africa based on bond ordering in paleosol carbonates. Proceedings of the National Academy of Sciences 107, 11245–11249.
Pfefferkorn, H.W., Mustafa, H., Hass, H., 1975. Quantitative charakterisierung ober-karboner abdruckfloren. Neues Jahrbuch für Geologie und Paläontologie (Abhandlungen) 150, 253–269.
Pfefferkorn, H.W., Gastaldo, R.A., DiMichele, W.A., Phillips, T.L., 2008. Pennsylvanian tropical floras of the United States as a record of changing climate. In: Fielding, C.R., Frank, T.D., Isbell, J.L. (Eds.), Resolving the Late Paleozoic Gondwanan Ice Age in Time and Space. Geological Society of America Special Paper, 441, pp. 305–316.
Quade, J., Eiler, J., Daeron, M., Achyathan, H., 2012. The clumped isotope geothermometer in soil and paleosol carbonate. Geochimica et Cosmochimica Acta 105, 92–107.
Roscher, M., Schneider, J.W., 2006. Permo-Carboniferous climate: Early Pennsylvanian to Late Permian climate development of central Europe in a regional and global context. In: Lucas, S.G., Cassinis, G., Schneider, J.W. (Eds.), Non-Marine Permian Biostratigraphy and Biochronology. Geological Society of London, Special Publication, 265, pp. 95–136.
Rygel, M.C., Fielding, C.R., Frank, T.D., Birgenheier, L.P., 2008. The magnitude of Late Paleozoic glacioeustatic fluctuations: a synthesis. Journal of Sedimentary Research 78, 500–511.
Savin, S.M., Hsieh, J.C.C., 1998. The hydrogen and oxygen isotope geochemistry of pedogenic clay minerals: principles and theoretical background. Geoderma 82, 227–253.
Savin, S.M., Lee, M., 1988. Isotopic studies of phyllosilicates. Reviews in Mineralogy 19, 189–223.
Sawin, R.S., West, R.R., Franseen, E.K., Watney, W.L., McCauley, J.R., 2006. Carboniferous–Permian boundary in Kansas, midcontinent, USA. Kansas Geological Survey, Bulletin 252, 1–13 (part 2).
Scheihing, M.H., 1980. Reduction of wind velocity by the forest canopy and the rarity of non-arborescent plants in the Upper Carboniferous fossil record. Argumenta Palaeobotanica 6, 133–138.
Sheldon, N.D., Tabor, N.J., 2009. Quantitative Paleoenvironmental and Paleoclimatic Reconstruction using paleosols. Earth Science Reviews 95, 1–52.
Tabor, N.J., 2007. Permo-Pennsylvanian palaeotemperatures from Fe-oxide and phyllosilicate $\delta^{18}O$ values. Earth and Planetary Science Letters 253, 159–171.
Tabor, N.J., Montañez, I.P., 2002. Shifts in Late Paleozoic atmospheric circulation over western equatorial Pangea: insights from pedogenic mineral $\delta^{18}O$ compositions. Geology 30, 1127–1130.
Tabor, N.J., Montañez, I.P., 2004. Permo-Pennsylvanian alluvial paleosols (north-central Texas): high-resolution proxy records of the evolution of early Pangean paleoclimate. Sedimentology 51, 851–884.
Tabor, N.J., Montañez, I.P., 2005. Oxygen and hydrogen isotope compositions of pedogenic phyllosilicates: development of modern surface domain arrays and implications for paleotemperature reconstructions. Palaeogeography, Palaeoclimatology, Palaeoecology 223, 127–146.
Tabor, N.J., Montañez, I.P., Southard, R.J., 2002. Mineralogical and stable isotopic analysis of pedogenic proxies in Permo-Pennsylvanian paleosols: implications for paleoclimate and paleoatmospheric circulation. Geochimica et Cosmochimica Acta 66, 3093–3107.

Tabor, N.J., Romanchock, C.M., Looy, C.V., Hotton, C.L., DiMichele, W.A., Chaney, D.S., 2013. Biome dynamics and niche-conservatism of Late Pennsylvanian vegetation in western equatorial Pangaea — climatic impact. Journal of the Geological Society (in press).

Urrego, D.H., Bush, M.B., Silman, M.R., Correa-Metrio, A., Ledru, M.-P., Mayle, F.E., Paduano, G., Valencia, B.G., 2009. Millennial-scale ecological changes in tropical South America since the Last Glacial Maximum. Developments in Paleoenvironmental Research 14, 283–300.

Wardlaw, B.R., 2005. Age assignment of the Pennsylvanian–Early Permian succession of North Central Texas. Permophiles 46, 21–22.

Webb III, T.S., Shuman, B., Williams, J.W., 2003. Climatically forced vegetation dynamics in eastern North America during the Late Quaternary Period. Development in Quaternary Science 1, 459–478.

White, D., 1936. Some Features of the Early Permian Flora of America. 16th International Geological Congress (1933) Proceedings, 1, pp. 679–689.

Williams, J.W., Shuman, B., Bartlein, P.J., Diffenbaugh, N.S., Webb III, T.S., 2010. Rapid, time-transgressive, and variable responses to early Holocene midcontinental drying in North America. Geology 38, 135–138.

Wilson, L.R., Rashid, M.A., 1975. Palynological evidence for a Pennsylvanian age assignment of the Gearyan series in Kansas and Oklahoma. In: Barlow, J.A. (Ed.), Proceedings of the First I. C. White Symposium "The Age of the Dunkard". West Virginia Geological and Economic Survey, Morgantown, WV, p. 183.

Wing, S.L., Harrington, G.J., Smith, F.A., Bloch, J.I., Boyer, D.M., Freeman, K.H., 2005. Transient floral change and rapid global warming at the Paleocene–Eocene boundary. Science 310, 993–996.

Yapp, C.J., 1990. Oxygen isotopes in iron (III) oxides: 1. Mineral-water fractionation factors. Chemical Geology 85, 329–335.

Yapp, C.J., 1993. The stable isotope geochemistry of low-temperature Fe(III) and Al "Oxides" with implications for continental paleoclimates. In: Swart, P.K., Lohmann, K.C., McKenzie, J., Savin, S. (Eds.), Climate Change in Continental Isotopic Records. Geophysical Monograph, 78, pp. 285–294.

Ziegler, A.M., Hulver, M.L., Rowley, D.B., 1997. In: Martini, I.P. (Ed.), Late Glacial and Post-Glacial Environmental Changes — Quaternary, Carboniferous-Permian and Proterozoic. Oxford University Press, Oxford, pp. 111–146.